Comparison of ray theory, Gaussian beam and finite difference modeling in 2-D media

Carlos A. S. Ferreira(*), João C. R. Cruz(*)
Centro de Geociências/CPGf/PROSIS, Universidade Federal do Pará, Brazil

Abstract

Gaussian beam (GB) methods have been used as a tool for modeling and imaging, due to its regularity in critical and caustic regions. We then use its features in the investigation of its sensitivities with respect to classical theories of modeling, such as ray theory and finite difference (FD) schemes. This is done by using a superposition of all GB's in the close vicinity of a specified receiver. Amplitudes are picked along synthetic sections of GB's and ray theory, and the results are compared to the ones derived from FD schemes. The results showed that GB predicts a smooth and continuous increase in amplitude, following the tendency of FD, while ray theory shows a sudden peak around the critical point of observation.

Introduction

In seismic methods, zero order ray theory has been widely used for modeling, migration and inversion problems. However, ray theory can only be effectively applied to smooth media, where the prevailing wavelength is much smaller than the characteristic structural dimensions we want to image. In this case, some phenomena, such as diffractions observed in complex geology settings, or in a laterally varying media, cannot be simulated adequately. Some other restrictions are related to the use of time-consuming two-point ray tracing algorithms and ocasional singularities inside the model. We mention some of these singularities in the cases of imaging fold flanks in salt domes and reflectors discontinuities, where generally are given rise to caustic observations and shadow zones.

The use of paraxial wavefields has been an attractive and efficient way of dealing with zero order ray theory limitations (Červenỳ, 1983). In general, these wavefields can be of real and complex nature. The real paraxial theory is widely known in the field of classical optics, while the complex paraxial theory is widely applied in quantum optics, where Gaussian beams are a well-known entity in laser propagation. In seismic imaging, the real paraxial theory has successfully been applied in stacking processing and is a key tool in true amplitude migration (Schleicher et al, 1993). On the other hand, complex paraxial theory is used for description of laterally varying wavefields in 2D and 3D media (Popov, 1996; Červenỳ, 1982*a*, 1982*b*) and migration methods (Hill, 2001).

One of the differences among the paraxial wavefields and zero order ray theory is the regularity description of the seismic field in singular regions. In fact, Gaussian beams are specially regular in regions of the wavefield where caustic prevail. Moreover, the Fermat principle based two point ray tracing is not needed, since in the case of the present paper the observed displacement on every record point is represented by a superposition of all paraxial wavefield in the vicinity of the receivers. The use of a dynamic ray tracing system allows in the determination of the paraxial amplitudes.

In this work we use all the features of the complex paraxial wavefield in a 2D homogeneous media in order to generate synthetic body wave seismograms composed of multi arrivals or a superposition of GB's. Some sensitivities parameters of the method are discussed with respect to the classical ray theory. We pick amplitudes along some GB's and ray synthetic seismograms and compare the results with the ones generated by a FD scheme.

Ray theory

In a perfectly elastic, isotropic, inhomogeneous media, the ray theory can be derived by solving the elastodynamic equation using the ray series (Červenỳ and Ravindra, 1971). If we consider frequency ω a large parameter, the leading order term of the ray series (n = 0) is of practical interest. By considering only the principal component of the compressional seismic wave and introducing the zero order ansatz

$$U_i(x_j,t) = U_i^{(0)}(x_j)\,\mathrm{e}^{-i\omega(t-\tau(x_j))}, \qquad (1)$$

where $\tau = \tau(\mathbf{x})$ is the traveltime, we derive the eikonal equation

$$\nabla\tau \bullet \nabla\tau = \frac{1}{\alpha(\mathbf{x})^2} \qquad (2)$$

where $\alpha = \alpha(\mathbf{x})$ is the *PP* wave velocity. The amplitude function satisfies the transport equation

$$2(\nabla\tau \bullet \nabla U^{(o)})\alpha + \alpha^2 U^{(0)} \nabla^2\tau + U^{(0)}(\nabla\tau \bullet \nabla\alpha^2) = 0 \qquad (3)$$

where "•" means inner product.

As can be seen, the solutions of (3) depend on the solutions of (2). Normally, this is not a easy task, and a better way of obtaining the solutions of (2) is using

characteristics (Bleistein, 1986; Bleistein et al, 1987), leading to the ray equations, which are ordinary differential equations of first order that are handled numerically using a Runge-Kutta algorithm. In 3D media the ray tracing system is given by

$$\frac{dx_i}{d\sigma} = p_i, \frac{dp_i}{d\sigma} = -v^{-3}\frac{\partial v}{\partial x_i}, \quad i = 1,2,3. \tag{4}$$

Here σ is a parameter measured along the ray, commonly related to the traveltime τ and to the arc length s according to

$$\sigma = \sigma_0 + \int_{s_0}^{s} v(s)\,ds = \sigma_0 + \int_{\tau_0}^{\tau} v^2(s)\,d\tau. \tag{5}$$

$v = v(x_i)$ is the velocity of propagation of the corresponding type of wave, while x_i are Cartesian coordinates of points of a ray and $p_i = \partial\tau/\partial x_i$ are Cartesian components of the slowness vector.

3D dynamic ray tracing

In order to understand the dynamic ray tracing (DRT) system, we must introduce two coordinate systems: the ray coordinate system (RCS) and the ray centred coordinate system (RCCS). Figure 1 depicts the situation in both cases.

In the RCS, given an initial curvilinear surface Σ, we select a ray $\Omega(\gamma_1,\gamma_2,\ \gamma_3 = s)$ passing through it, where coordinates γ_1, γ_2 are specified along the surface and γ_3 is considered along the ray, perpendicular to the initial surface. In the RCCS system, given an arbitrary ray Ω initiated at some point S_γ on the surface Σ, we fix some point along its arc length, say R_γ, and form a 2D orthogonal coordinate system, whose components are q_1 and q_2, in a plane $\Sigma^\perp$ perpendicular to the ray at $q_3 = s$. In this way, a point **R'** situated in the close vicinity of the ray and on the plane $\Sigma^\perp$ has as position vector $\mathbf{r}(q_1,q_2,s) = \mathbf{r}(0,0,s) + q_1\mathbf{e}_1 + q_2\,\mathbf{e}_2$, where $\mathbf{e}_1$ and $\mathbf{e}_2$ are basis vectors situated on the plane $\Sigma^\perp$**.** The third basis vector $\mathbf{e}_3 = \mathbf{t}$ coincides with the slowness vector at R_γ.

Using the RCCS system, we introduce the DRT system as

$$d\,\mathbf{Q}/ds = v^{-2}\,\mathbf{P}, \qquad d\,\mathbf{P}/ds = -v\,\mathbf{V}\mathbf{Q} \tag{6}$$

where **Q**, **P** and **V** are 2x2 matrices with components defined by

$$Q_{IJ} = \left.\frac{\partial q_I}{\partial \gamma_J}\right|_{q_1,q_2=0}, P_{IJ} = \left.\frac{\partial p_I}{\partial \gamma_J}\right|_{q_1,q_2=0}, V_{IJ} = \left.\frac{\partial^2 v}{\partial q_I\,\partial q_J}\right|_{q_1,q_2=0}.$$

$I, J = 1, 2$ (7)

V = **V**(s) is a 2x2 matrix whose elements represent second mixed derivatives of the velocity field in ray centred coordinates and $v = V(0,0,s)$ is the velocity along the ray. Mathematically, **Q** is a transformation matrix from ray coordinates to centred coordinates and **P** is a transformation matrix from the ray coordinates to slowness components ray coordinates. Physically, **Q** is referred to as the matrix of geometrical spreading, while **P** has a non obvious physical meaning. In this way we define a 2x2 matrix **M** of second derivatives of the traveltime field with respect to the ray centred coordinates

$$M_{IJ} = \left.\frac{\partial^2\tau}{\partial q_I\,\partial q_J}\right|_{q_1,q_2=0} \tag{8}$$

which is equivalent to writing $\mathbf{M}(s) = \mathbf{P}\mathbf{Q}^{-1}$, evaluated along the ray.

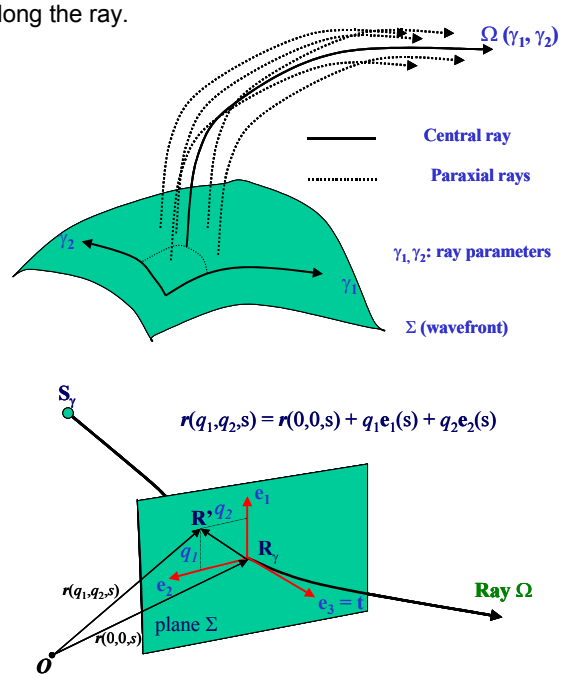

Figura 1 – Ray coordinates (top) and ray centred coordinates (bottom).

Gaussian beam theory

By definition, Gaussian beams (GB's) are the high-frequency asymptotic time-harmonic solutions of elastodynamics equations concentrated close to their rays (Klimeš, 1984). It is most naturally written in orthogonal ray-centred coordinates, where the polarization of the beams does not change along this coordinate system.

Let us consider only *PP* waves and take in consideration an arbitrary ray Ω. In the close vicinity of such a ray, we construct an approximate solution of the elastodynamic equation that fulfills the following conditions: 1) the solution is concentrated close to the central ray and its amplitudes decrease exponentially with the increasing distance from the central ray; and 2) it should have no singularities along the ray. If the two previous conditions

are satisfied and we use the solutions of the DRT system previously discussed, the complex-valued vector amplitude is given by

$$\mathbf{U}(R,\omega) = \frac{\Lambda_0 \ \vec{\mathbf{t}}}{\sqrt{det\,\mathbf{Q}(s)}} \times exp[i\,\omega(\tau(s) + \frac{1}{2}\mathbf{q} \bullet \mathbf{M}\mathbf{q})] \quad (9)$$

where Λ_0 is an initial amplitude factor. Equation (9) is the approximate solution of the elastodynamic equation in the vicinity of the central ray and is commonly known as Gaussian beam, where **t**(*s*) is the tangent unit vector along the ray. When dealing with GB's, some conditions must be fulfilled by (9). The first is Im(**M**) > 0, which garantees the concentrations of all rays around the central ray. Once this first condition is obeyed, the second condition states that *det*(**Q**(*s*)) ≠ 0, which means that the wavefield described by GB's are regular even in singular regions, no matter how complex the medium may be.

Gaussian beam superposition integral

Following the features studied in the former sections, we determine the elementary wavefield $U_i(R,\omega)$ observed on a fixed receiver *R*, here described in the frequency domain. If zero order ray theory is used, rays need to be traced using a velocity model in a specified medium, and its paths and traveltimes are searched for each fixed source-receiver pair. This procedure is known as two point ray tracing and is time consuming (Červenỳ et al, 1982*b*). If, on the other hand, paraxial wavefields are used, the same procedure can be executed without a ray $\Omega(\gamma_1, \gamma_2, s)$ ever hitting the observation point *R*. Here γ_1 and γ_2 are any ray parameters used to describe the central ray, e.g, take-off angles. Instead, the wavefield is calculated by a weighted paraxial superposition of rays connected with a central ray in the vicinity of the observation point *R*. This avoids two point ray tracing. In this way, the wavefield is obtained by a superposition integral, in the frequency domain, given by (Červenỳ, 2000)

$$U_i^{(x)}(R,\omega) = \int_D d\gamma_1\, d\gamma_2\, \Phi(\gamma_1,\gamma_2) U_i^{(x)}(R_\gamma)\, exp[i\,\omega T(R,R_\gamma)] \quad (10)$$

where $U_i^{(x)}(R,\omega)$ is the Cartesian component of the displacement vector at receiver *R*, *D* denotes the region of ray parameters in consideration and $\Phi(\gamma_1,\gamma_2)$ is a weighting factor that is determined asymptotically. Klimeš (1984) determines Φ using a geometrical interpretation, based on the expansion of the wavefield given on an initial surface. His result is similar to the one found asymptotically by Červenỳ (2000). We consider that the point R_γ belongs to the same ray as point S_γ, where the ray began, close enough to a fixed point *R*. Finally, $U_i^{(x)}(R_\gamma)\exp[i\,\omega T(R,R_\gamma)]$ represents the GB's connected to the central ray Ω, where $T(R,R_\gamma)$ is the paraxial traveltime at *R* due to the traveltime of a ray at R_γ.

In (10) the amplitude factor can be decomposed in two components:

$$U_i^{(x)}(R_\gamma) = U^{\Omega}(R_\gamma)\sqrt{det\,\mathbf{Q}(S_\gamma)/det\,\mathbf{Q}(R_\gamma)} \quad (11)$$

and

$$U^{\Omega}(R_\gamma) = \sqrt{\rho(S_\gamma)v(S_\gamma)/\rho(R_\gamma)v(R_\gamma)}\,R^c\,g_i(R_\gamma)\,. \quad (12)$$

The factor (12), called the spreading free amplitude, is constituted by terms related to the ray itself (density, phase velocities at initial and end points of the ray, normalized transmission/reflection coefficient factors along the ray, polarization vectors, etc), and a spreading dependent factor (11), which embodies the geometrical spreading factor and phase shifts due to caustics and due to some other factors, e.g., phase shift due to the source (Červenỳ, 2000).

In the construction of synthetic seismograms in this paper we have used equation (10), reduced to the 2D case

$$U_i^{(x)}(R,\omega) = \int_{\phi_{min}}^{\phi_{max}} d\phi\,\Phi(\phi) U_i^{(x)}(R_\phi)\, exp[i\,\omega T(R,R_\phi)], \quad (13)$$

where ϕ_{min} and ϕ_{max} are the angular (zenital) opening (since the ray parameter chosen to describe the rays are the take-off angles derived from a explosive point source) and $\Phi(\phi)$ is the weighting function related to the initial conditions at the source. In a 2D homogeneous media, this function is given by (Červenỳ, 2000; Klimeš, 1984; Popov, 1996)

$$\Phi = \sqrt{\frac{\omega}{2\pi}}\ \sqrt{\frac{1}{v(s)l(s)}}\ |l(s)| \quad (14)$$

where function $l(s) = (s - s_0)$, with *s* and s_0 being the final and initial arclength along the ray, respectively, and $v(s) = v_0$.

We have chosen to compute integral (13) in the time domain. By Fourier transforming (13) only for positive values of frequency and interchanging the order of integration, (13) becomes the wave packet approach (Červenỳ, 1983; Beydoun and Keho, 1987)

$$U_i^{(x)}(R,t) = f(t) * (\frac{1}{\pi})\,\mathrm{Im}[\int_{\phi_{min}}^{\phi_{max}} d\phi \frac{\Phi(\phi) U_i^{(x)}(R_\phi)}{t - T(R,R_\phi)}], \quad (15)$$

where "*" means convolution, *f*(*t*) is the source function and "Im" means the "imaginary part of". As can be noticed, (15) has an non-oscillatory form and a single kernel to be evaluated. Together with definition (13) and with the use of a causal Gabor wavelet, equation (15) leads to the use of an analytical signal.

Some comments must be made with respect to some factors appearing in (15). The paraxial traveltime $T(R,R_\phi)$ is calculated using general Cartesian coordinates for a 2D case (Klimeš, 1984)

$$T(R,R_\phi) = T(R_\phi) + p_I(x_I - \tilde{x}_I) + \\ + (1/2)(x_I - \tilde{x}_I)(x_J - \tilde{x}_J)(H_{IK}H_{JL}M_{KL}), \quad (16)$$

(I, J, K, L = 1, 2) where x_I are the observations points coordinates and $\tilde{x}_I$ are the coordinates of the termination points of the central rays. The components of matrix **H** represent cosine directors when transforming from the ray centred coordinates to general Cartesian coordinates.

Examples

The complex paraxial wavefield superposition was tested in a 2D homogeneous medium restricted to the in-plane *xz*. A geological model composed of a layer over a half space is considered, where a horizontal reflector is imersed in an constant velocity overburden. The dimensions considered are: horizontal length of 2.0 km and a total depth of 2.0 km. A plane refletor is located at depth 1.0 km. Only *P* wave velocities are considered: 2.0 km/s and 3.5 km/s, above and bellow the reflector, respectively. This contrast in velocity was chosen in such a way that a critical angle of reflection may occur at 35^0, giving rise to a critical region inside the model. A group of 80 receivers are located on the surface, on the right side of the coordinate system origin. The distance between each receiver is 25 m. Figure 2 shows a sketch of the geological model together with its ray diagram. We have chosen as acquisition geometry a common shot gather.

Figure 3 depicts a comparison between the resulting seismograms using zero order ray theory and equation (15), respectively. We notice that due to the critical reflection angle, the reflection coefficient becomes imaginary and the waveform observed around x = 1400 m in Figure 3 (bottom) exhibits a 90° phase change. When the GB superposition is used (Figure 3, top), the same behavior is smoothed in the critical observation point. The dominant frequency used in both cases was 5 Hz and the GB seismogram was obtained using 200 wave packets. In this respect, we have made extensive tests with different number of packets, as well as with varying frequencies, and decided that the present number of packets was sufficient to describe the wavefield adequately, using the frequency mentioned above. This is an inherent characteristic of the GB approach, as Červenỳ (1983) showed using a similar model like the one depicted in Figure 2, and depends on how “high” is the dominant frequency for the model in consideration. Also, since the beam half width is frequency dependent, it is reasonable to expect a direct relationship between the number of packets used in the construction of synthetic seismograms and the dominant frequency, in order to calculate the amplitudes for each receiver accurately.

In Figure 4 we depict the FD seismogram with a reflection event at *P1* (red arrow). This FD seismogram was obtained with a grid spacing of Δx = 25 m and time sampling of Δt = 1 ms, for a dominant frequency of 5 Hz. We have made use of the FD program FDSKALAR (Sandmeier & Liebhardt, 1992) for generating the synthetic seismogram.

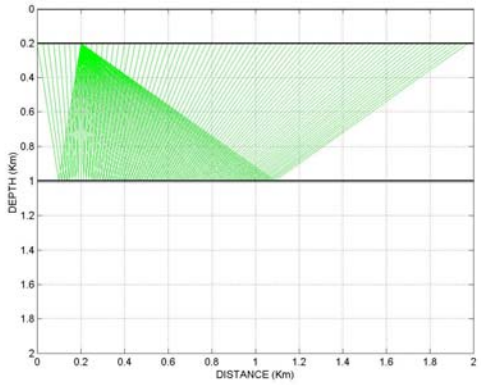

Figure 2 - 2D sketch of geological model and ray diagram in a common shot geometry. A critical angle occurs at approximately 35^0.

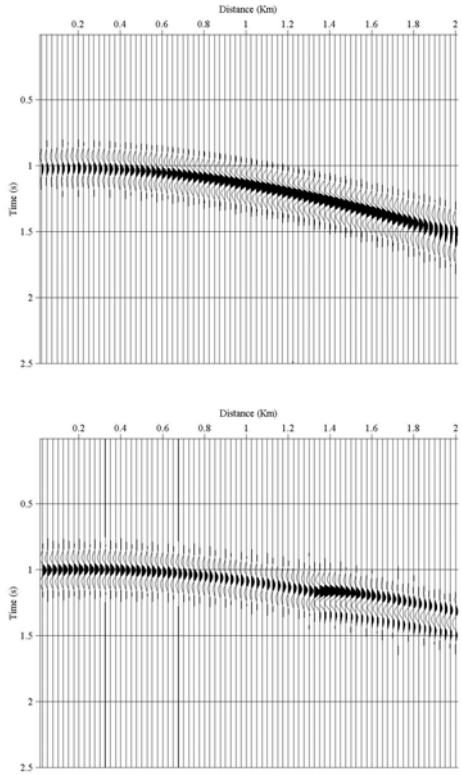

Figure 3 – *Top*: Gaussian beam (wave packet) seismogram. Total number of wave packets used N = 200. *Bottom*: Zero order ray theory seismogram.

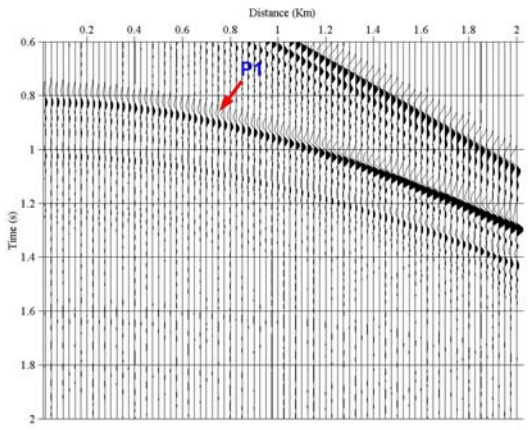

Figure 4 – FD seismogram showing P1, the principal event of interest, corresponding to the primary reflections.

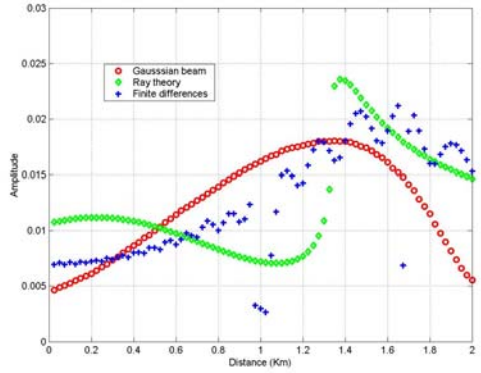

Figure 5 – Comparison of amplitude pickings: ray theory (green diamonds), Gaussian beam (red circles) and FD (blue crosses).

In Figure 5 we have picked amplitudes along both ray and GB's sections and compared the results with the ones derived from a finite difference modeling scheme. In the comparisons, we have maintained the previous parameters and fixed the number N = 200 of packets and dominant frequency of 5 Hz to be analysed. The analysis is of importance due to the behaviour of amplitudes in the critical region. While the ray theory (green diamonds) predicts a smooth decrease in amplitudes followed by a sudden peak around the critical point, the GB theory (red circles) predicts a smooth and continuous increase, whereas FD theory (blue crosses) behaves with the same tendency but with some discontinuities (outliers) along the whole section. In this manner, GB seems to fit better with respect to FD than ray theory.

Conclusions

We have tested the use of paraxial Gaussian beams in order to obtain synthetic body wave seismograms in a 2D media composed of one layer over a half space, in a homogeneous velocity overburden. The velocity contrast was chosen in such a way as to yield a critical angle of reflection of 35°, for a critical observation point located at x = 1400 m. Our results showed that while the ray theory synthetic seismogram showed a 90° phase change in the critical observation point, the GB seismogram smoothed the amplitudes around the same point. Several tests with a varying number of rays, as well as varying frequencies, showed that a dense fan of rays must be used in order to get seismograms with sufficient accuracy. A frequency of 5 Hz was used when the comparison of both ray theory and GB approach was extended to the amplitudes derived from a modeling scheme using finite differences. The GB picked amplitudes showed a smooth and continuous increase, following the tendency of the FD scheme, while the ray theory picked amplitudes presents a smooth decrease followed by a sudden peak around the critical point.

Acknowledgements

The first author thanks the Brazilian National Research Council (CNPq) for his PhD scholarship during all stages of this research. He thanks Prof. Martin Tygel for the support and friendship during his stay at IMECC/Unicamp, Brazil, for six months. He is grateful to Prof. Jörg Schleicher for all fruitful discussions during the course on seismic imaging theory at IMECC/Unicamp. Vlastislav Červený and Ludek Klimeš are also acknowledged for their constructive suggestions. Ludek Klimeš was very kind by making available some papers of his own on Gaussian beams.

References

Beydoun, W. B.; Keho, T. H., 1987. The paraxial ray method. Geophysics, **52**, 1639-1653.

Bleistein, N., 1986. Two and one half dimensional in plane wave propagation. Geophys. Prosp., **3**4, 686-703.

Bleistein, N.; **Cohen, J. K.; Hagin, F. G**., 1987. Two and one half dimensional Born inversion with an arbitrary reference. Geophysics, **52**,26-36.

Červený, V.; Ravindra, R., 1971. Theory of seismic head waves. University of Toronto Press.

Červený, V., 1982. Expansion of a plane wave into Gaussian beams. Studia Geoph. Et. Geod., **26**, 120-131.

Červený, V.; **Popov, M. M.; Psencik, I.**, 1982. Computations of wavefields in inhomogeneous media.

Červený, V., 1983. Synthetic body wave seismogram for laterally varying layered structures by the Gaussian beam method. Geophys. J. R. astr, Soc., **73**, 389-426.

Červený, V., 2000. Summation of paraxial Gaussian beams and of paraxial ray approximations in inhomogeneous anysotropic layered structures. In:

Seismic Waves in Complex 3D Structures, Report 10. Charles University, Prague, 121-159.

Hill, N. R., 2001. Prestack Gaussian beam depth migration. Geophysics, **66**, 1240-1250.

Klimeš, L., 1984. Expansion of a high frequency time harmonic wavefield given on a initial surface into Gaussian beams. Geophys. J. R. astr. Soc., **79**, 105-118.

Popov, M. M., 1996. Ray theory and Gaussian beam method for geophysicists. PPPG, UFBA, 148p.

Sandmeier, M. M.; Liebhardt, G. H., 1992**.** Software Refra. Geophysical Institute of Karlsruhe University. Gemany.

Schleicher, J.; Tygel, M.; Hubral, P., 1993. 3-D true-amplitude finite-offset migration: Geophysics, 58, 1112--1126.